

Electroweak corrections in Drell–Yan production

A. Huss^{1,2}, M. Schönherr²

¹ Institute for Theoretical Physics, ETH, CH-8093 Zürich, Switzerland

² Department of Physics, University of Zürich, CH-8057 Zürich, Switzerland

Abstract

We compare the description of higher-order electroweak corrections at $\mathcal{O}(\alpha)$ and $\mathcal{O}(\alpha_s\alpha)$ in Drell–Yan production.

1. Introduction

The Drell–Yan-like production of electroweak gauge bosons represents one of the key Standard Model processes at hadron colliders whose detailed understanding is crucial in order to exploit the full potential of the measurements performed at the LHC. The neutral-current process $pp \rightarrow Z/\gamma \rightarrow \ell^+\ell^-$, in particular, has a very clean experimental signature owing to the two charged leptons in the final state which further allows for the full reconstruction of the kinematics of the intermediate gauge boson. Not only does this process constitute a powerful tool for detector calibration, but it also delivers important constraints in the fit of PDFs and allows for precision measurements such as the extraction of the weak mixing angle $\sin^2(\theta_{\text{eff}}^\ell)$.

On the theory side, Drell–Yan production belongs to one of the most precisely predicted processes: QCD corrections are known up to NNLO [1] and the NLO electroweak (EW) corrections have been computed as well. Until recently, the largest missing piece in terms of fixed-order predictions were given by the NNLO mixed QCD–EW corrections. Different approaches of combining QCD and EW corrections revealed that the missing $\mathcal{O}(\alpha_s\alpha)$ corrections could have an impact of a few per cent in the resonance region, i.e. at the level that is relevant for precision phenomenology. In a series of papers [1, 2], the calculation of these corrections have been tackled using the so-called pole approximation (PA). This approach is suitable to describe observables that are dominated by resonances and the computation of the numerically most important contribution has been performed in Ref [2].

In this work, we investigate how the $\mathcal{O}(\alpha_s\alpha)$ corrections generated through a parton-shower approach compares to the result of Ref[1]. Section 2. gives a brief overview of the computation employing the PA and the implementation of the QED shower in the SHERPA Monte Carlo program [3]. In Sect. 3. we present our numerical results of the comparison before we conclude in Sect. 4..

2. Computation

The Pole approximation: The calculation of the $\mathcal{O}(\alpha_s\alpha)$ corrections in Refs. [1, 2] was performed in the framework of a pole expansion, which is based on a systematic expansion of the cross section around the gauge-boson resonance $p_V^2 \sim \mu_V^2$, with $\mu_V^2 = M_V^2 - iM_V\Gamma_V$ denoting the gauge-invariant location of the propagator pole in the complex plane. Only retaining the leading contributions that are enhanced by a resonant propagator, we obtain the so-called pole approximation (PA). As a result of applying the PA, the calculation is split into separate well-defined parts that can be classified into the non-factorizable and factorizable corrections: The non-factorizable corrections involve soft-photon exchange between the production and decay stages of the process and constitute the conceptually most difficult part of the calculation. They have been computed in Ref. [1] and were found to be negligible for all phenomenological purposes. The factorizable contributions involve corrections where the production of the intermediate gauge boson and its decay proceed independently. Here, the factorizable corrections of “initial–final”

reference to a section adds an additional “.”

better section title

type were identified as the numerically dominant contribution—combining the sizeable QCD corrections to the production sub-process with the large EW corrections of the gauge boson decay—which were computed in Ref. [2]. The remaining factorizable corrections are given by the “initial–initial” and “final–final” types. The latter were found to be numerically negligible [2], while the former are not expected to deliver a sizeable correction, in particular for observables that are less sensitive to initial-state radiation effects. In the remainder of this work, we will thus focus our attention to the initial–final factorizable corrections which we will often simply refer to as the $\mathcal{O}(\alpha_s\alpha)$ corrections in the PA. More details on the calculation of the $\mathcal{O}(\alpha_s\alpha)$ corrections in the PA is given in Refs. [1, 2].

The QED shower in Sherpa: Another approach to higher order QED or electroweak corrections is presented in the soft-photon resummation of Yennie, Frautschi and Suura (YFS) [4]. Therein the universal structure of real and virtual soft photon emissions is exploited to construct an all-order approximation to the process at hand which can be systematically supplemented with process-dependent finite hard real and virtual emission corrections. The implementation presented in Ref. [5] focusses on higher-order QED corrections to particle decays and is used since as the default mechanism for such corrections in SHERPA [3], both for elementary particle (e.g. W^\pm , Z , τ^\pm) as well as hadron decays.

In the present context of lepton pair production the higher-order QED corrections are effected in a factorised approach. The complete process $pp \rightarrow \ell^+\ell^-$ is calculated at LO or NLO in the strong coupling constant keeping all off-shell effects. Then, an intermediate resonance X is reconstructed from the lepton pair and assigned its invariant mass. Its decay width is then corrected for higher order QED corrections, including YFS resummation, to

$$\Gamma = \frac{1}{2m_X} \sum_{n_\gamma=0}^{\infty} \frac{1}{n_\gamma!} \int d\Phi e^{Y(\Omega)} \prod_{i=1}^{n_\gamma} d\Phi_i \tilde{S}(k_i) \Theta(k_i, \Omega) \left[\tilde{\beta}_0^0 + \tilde{\beta}_0^1 + \sum_{i=1}^{n_\gamma} \frac{\tilde{\beta}_1^1(k_i)}{\tilde{S}(k_i)} + \mathcal{O}(\alpha^2) \right]. \quad (1)$$

Therein, m_X is the mass of the decaying resonance and $d\Phi$ is the phase element of the leading order decay, and $\tilde{\beta}_0^0$ is the leading order decay squared matrix element. The $Y(\Omega)$ then is the sum of the eikonal approximations to virtual photon exchange and unresolved soft real photon emission, Ω denoting the region in which soft photons are not resolvable. The YFS form factor, $e^{Y(\Omega)}$ then resums these leading logarithmic universal corrections to all orders. Resolved photons are then described explicitly, emission by emission, by the eikonal \tilde{S} depending on the individual photon momentum k_i . $d\Phi_i$ is the corresponding phase space element. The eikonal approximations used in both the YFS form factor and for resolved real emissions can then, order-by-order, be corrected by supplementing the corresponding infrared-subtracted squared matrix elements $\tilde{\beta}_i^{i+j}$ of $\mathcal{O}(\alpha^{i+j})$ relative to the Born decay and containing i resolved photons. Since all charged particles are considered massive in the context of YFS resummation, all $\tilde{\beta}_i$ are free of any infrared singularity. Finally, it is interesting to note that in the case of multi-photon emission each emitted photon receives the hard emission correction $\tilde{\beta}_1^1$ in the respective one-photon emission projected phase space.

The implementation used here, as we restrict the γ^*/Z propagator virtuality to be near the Z mass, always identifies the resonance X with the Z boson. The calculation thus contains the $\mathcal{O}(\alpha)$ virtual corrections $\tilde{\beta}_0^1$ and real emission corrections $\tilde{\beta}_1^1$ resulting in an NLO QED accurate description. As NLO weak corrections are finite they can in principle be incorporated in the $\tilde{\beta}_0^1$. This is left to a future work.

3. Results

The numerical results presented in this section are obtained using the same input parameters and event selection cuts as in Ref. [2]. The electroweak coupling constant α is defined in the G_μ -scheme, with the exception of the photonic corrections which use $\alpha(0)$ as their coupling. All results are obtained using the NNPDF2.3QED NLO PDF set [6], in particular, also the LO predictions shown in the following

were evaluated using this PDF set. For the charged leptons in the final state we consider two different reconstruction strategies: In the case of “dressed” leptons we apply a photon recombination procedure in order to treat all collinear lepton–photon configurations inclusively, whereas in the “bare” muon setup no such recombination is performed. Further details on the calculational setup and the event reconstruction are given in Ref. [2].

In order to establish the setup of the two computations, we first consider the $\mathcal{O}(\alpha)$ corrections by applying the YFS shower in SHERPA to the LO prediction, $\sigma_{\text{Sherpa}}^{\text{LO}\otimes\text{YFS}}$, and comparing it to the full EW corrections denoted as $\sigma^{\text{NLO[EW]}}$ ¹. The respective relative correction factors, normalised to the LO prediction, are then given by

$$\delta_{\alpha}^{\text{Sherpa}} = \frac{\sigma_{\text{Sherpa}}^{\text{LO}\otimes\text{YFS}} - \sigma^{\text{LO}}}{\sigma^{\text{LO}}}, \quad \delta_{\alpha} = \frac{\sigma^{\text{NLO[EW]}} - \sigma^{\text{LO}}}{\sigma^{\text{LO}}}. \quad (2)$$

For the mixed QCD–EW corrections, we generate terms of $\mathcal{O}(\alpha_s\alpha)$ by applying the QED shower on top of the fixed-order NLO QCD prediction, which we denote by $\sigma_{\text{Sherpa}}^{\text{NLO[QCD]}\otimes\text{YFS}}$. These results are compared to the best prediction of Ref. [2], $\sigma_{\text{PA}}^{\text{NNLO[QCD}\times\text{EW}]}$, which includes the full NLO QCD and EW corrections, supplemented by the dominant $\mathcal{O}(\alpha_s\alpha)$ corrections in the PA. In order to extract the genuine $\mathcal{O}(\alpha_s\alpha)$ contribution from the prediction based on the YFS shower, we define the relative correction factor as follows,

$$\delta_{\alpha_s\alpha}^{\text{Sherpa}} = \frac{(\sigma_{\text{Sherpa}}^{\text{NLO[QCD]}\otimes\text{YFS}} - \sigma^{\text{NLO[QCD]}}) - (\sigma_{\text{Sherpa}}^{\text{LO}\otimes\text{YFS}} - \sigma^{\text{LO}})}{\sigma^{\text{LO}}}. \quad (3)$$

For the fixed-order prediction in the PA, the corresponding correction factor is given by

$$\delta_{\alpha_s\alpha}^{\text{PA}} = \frac{\sigma_{\text{PA}}^{\text{NNLO[QCD}\times\text{EW}]} - \sigma^{\text{NLO[QCD+EW]}}}{\sigma^{\text{LO}}}. \quad (4)$$

The numerical results comprise differential distributions in the lepton invariant mass $m_{\ell\ell}$, the transverse momentum of the positively charged lepton $p_T^{\ell^+}$, and the rapidity of the lepton pair $y_{\ell\ell}$, which are shown in Figs. 1–3, respectively. The left plot in the figures shows a comparison of the NLO EW corrections, while the right-hand plot compares the corresponding $\mathcal{O}(\alpha_s\alpha)$ corrections. In each plot we show the absolute distributions in the top frame and the relative correction factors in the bottom panel as defined in Eq. (2) for the $\mathcal{O}(\alpha)$ and Eqs. (3) and (4) for the mixed QCD–EW corrections.

For the invariant mass distribution shown in Fig. 1 we observe an overall good agreement between the QED shower and the fixed-order result. This reflects the property of this observable whose corrections are known to be dominated by final-state photon emission. Both at $\mathcal{O}(\alpha)$ and $\mathcal{O}(\alpha_s\alpha)$ we observe a small offset between the two predictions where the parton-shower approach leads to slightly smaller corrections below the Z resonance. This difference originates from multi-photon emissions, which is included in the YFS shower (1) whereas the fixed-order prediction is restricted to at most one photon emission. Figure 2 shows the corrections to the transverse momentum distribution of the positively charged lepton, $p_T^{\ell^+}$. Although giving qualitatively a similar shape in the $\mathcal{O}(\alpha)$ corrections, we observe larger differences between the two computations around the resonance and in the higher transverse momentum tails. This difference can be understood from the fact that this observable is sensitive to initial-state radiation effects, which are not accounted for in the shower approach. Indeed, comparing the final-state factorizable $\mathcal{O}(\alpha)$ corrections in PA to the full NLO EW corrections shows a very similar picture as seen here (see Fig. 9 in Ref. [1]). For the mixed-QCD–EW corrections, on the other hand, the EW corrections contained in the $\mathcal{O}(\alpha_s\alpha)$ PA prediction are also confined to the decay sub-process similarly to the case of the QED shower. As a result, we see a much better agreement between the two computations here. Lastly, the

¹A comparison of the PA at $\mathcal{O}(\alpha)$ against the full NLO EW corrections has been performed in Ref[1].

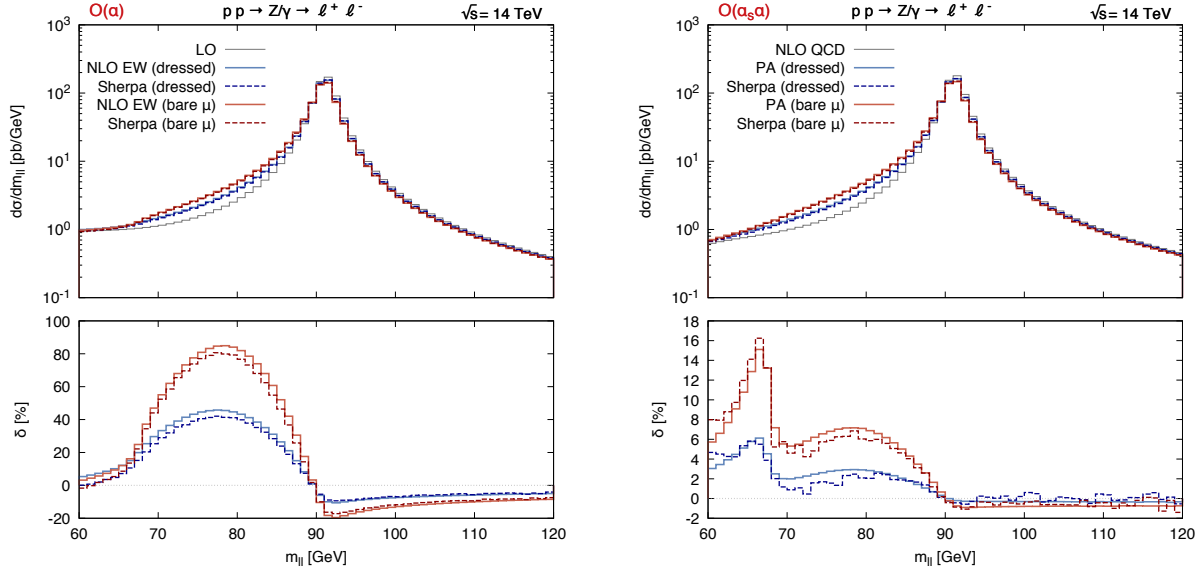


Fig. 1: Comparison of the $\mathcal{O}(\alpha)$ (left) and $\mathcal{O}(\alpha_s \alpha)$ (right) corrections to the invariant-mass distribution of the lepton pair $m_{\ell\ell}$ between Ref. [2] and Sherpa. The absolute distributions and the relative corrections at the respective order are shown in the top and bottom panels, respectively. Collinear lepton–photon configurations are treated both inclusively with a recombination procedure resulting in the “dressed” setup (blue) or exclusively in the case of muons labelled as “bare μ ” (red).

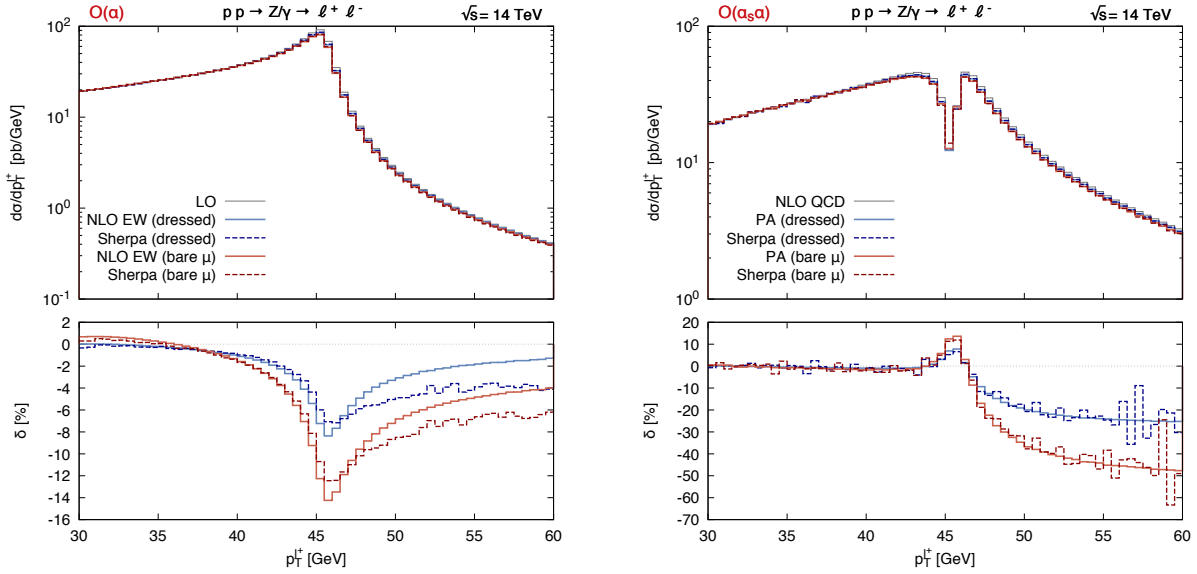


Fig. 2: Comparison of the $\mathcal{O}(\alpha)$ (left) and $\mathcal{O}(\alpha_s \alpha)$ (right) corrections to the transverse-momentum distribution of the positively charged lepton $p_T^{\ell^+}$ between Ref. [2] and Sherpa. The absolute distributions and the relative corrections at the respective order are shown in the top and bottom panels, respectively. Collinear lepton–photon configurations are treated both inclusively with a recombination procedure resulting in the “dressed” setup (blue) or exclusively in the case of muons labelled as “bare μ ” (red).

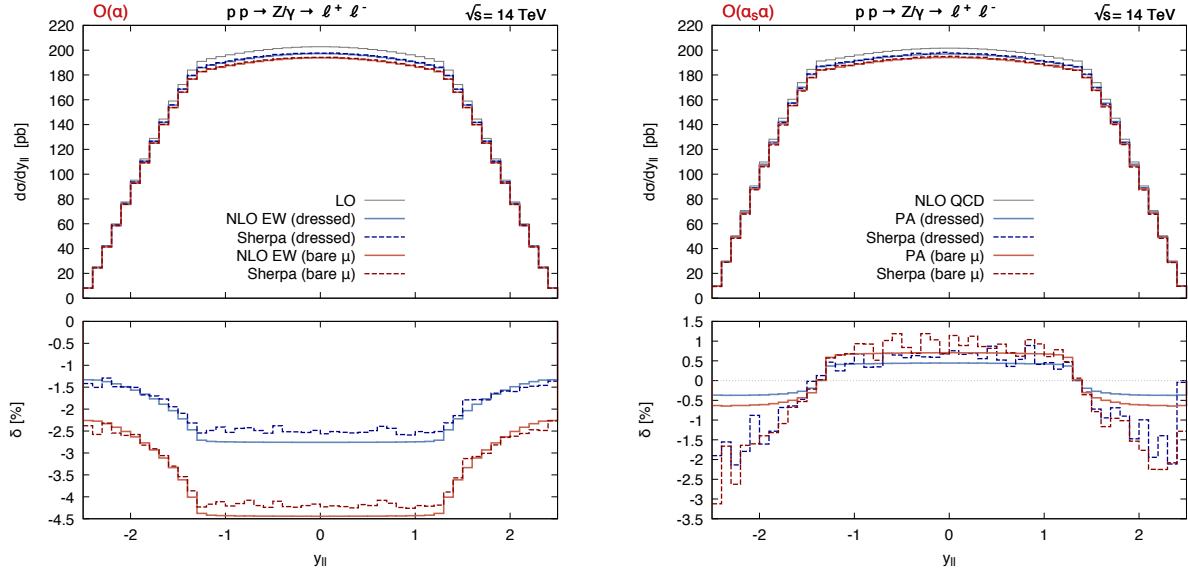


Fig. 3: Comparison of the $\mathcal{O}(\alpha)$ (left) and $\mathcal{O}(\alpha_s \alpha)$ (right) corrections to the rapidity distribution of the lepton pair $y_{\ell\ell}$ between Ref. [2] and Sherpa. The absolute distributions and the relative corrections at the respective order are shown in the top and bottom panels, respectively. Collinear lepton–photon configurations are treated both inclusively with a recombination procedure resulting in the “dressed” setup (blue) or exclusively in the case of muons labelled as “bare μ ” (red).

numerical results for the rapidity distribution of the lepton pair $y_{\ell\ell}$ are shown in Fig. 3. At $\mathcal{O}(\alpha)$, the shower prediction is able to reproduce the exact fixed-order result to a large extent up to a small offset in the normalisation. This shift can be attributed to the finite weak corrections which are missing in the YFS shower prediction. The purely weak corrections amount to a constant correction of approximately -0.5% in this distribution which precisely matches the observed offset. For the mixed QCD–EW corrections we obtain corrections from the QED shower that are similar in shape to those of the fixed-order prediction in the PA, however, with larger negative corrections in the forward regime.

any simple explanation for this?

4. Conclusions and outlook

The Drell–Yan process is one of the most important “standard candle” processes at the LHC and, as such, has a wide range of applications. In this work, we have explored the possibility of generating mixed QCD–EW corrections of $\mathcal{O}(\alpha_s \alpha)$ to this process using the YFS shower available in the SHERPA Monte Carlo and performed a comparison to the fixed-order calculation of Ref. [2]. To this end, we have considered both $\mathcal{O}(\alpha)$ and $\mathcal{O}(\alpha_s \alpha)$ corrections to various differential distributions given by the invariant mass of the leptons, the lepton transverse momentum, and the rapidity of the lepton pair. We find that the QED shower is able to capture the electroweak corrections to these observables remarkably well and we were further able to identify the sources for the small differences that was observed between the two predictions.

Building on the insights that were gained from this study, it will be interesting to investigate further observables and also repeating this comparison for the charged-current process. Furthermore, potential improvements were identified in both computations which should be explored in order to gain more insight into the numerical impact of the various ingredients that enter the two predictions. Such improvements include the finite weak corrections that can be incorporated to the YFS shower approach through the $\tilde{\beta}^1$ coefficient in Eq. (1) on the one side, and supplementing the fixed-order calculation with multi-photon emission effects.

ACKNOWLEDGEMENTS

We thank the organisers.

References

- [1] S. Dittmaier, A. Huss, and C. Schwinn, *Nucl. Phys.* **B885** (2014) 318–372, [1403.3216].
- [2] S. Dittmaier, A. Huss, and C. Schwinn, *Nucl. Phys.* **B904** (2016) 216–252, [1511.08016].
- [3] T. Gleisberg, S. Höche, F. Krauss, M. Schönherr, S. Schumann, and J. Siegart, F and Winter, *JHEP* **02** (2009) 007, [0811.4622].
- [4] D. R. Yennie, S. C. Frautschi, and H. Suura, *Ann. Phys.* **13** (1961) 379–452.
- [5] M. Schönherr and F. Krauss, *JHEP* **12** (2008) 018, [0810.5071].
- [6] R. D. Ball *et. al.*, *Nucl.Phys.* **B867** (2013) 244–289, [1207.1303].